Urquiza Villalonga, David Alejandro; Fernández-Getino García, M. Julia. (2020). Performance comparison of interference alignment algorithms in an energy harvesting scenario. *12th IEEE/IET International Symposium on Communication Systems, Networks and Digital Signal Processing, (CSNDSP), 20-22, July 2020* (Online), [6] pp.

Performance comparison of interference alignment algorithms in an energy harvesting scenario

David Alejandro Urquiza Villalonga
Department of Signal Theory and Communications, Carlos III University of Madrid
28911, Leganés, Madrid, Spain,
daurquiza@tsc.uc3m.es

M. Julia Fernández-Getino García
Department of Signal Theory and Communications, Carlos III University of Madrid
28911, Leganés, Madrid, Spain,
mjulia@tsc.uc3m.es

***Abstract*—Energy-efficient interference alignment (IA) algorithms that simultaneously satisfy continuous coverage and green communications requirements are an open problem in 5G cellular networks. IA is one of the most promising techniques to eliminate interference. However, a recent assumption in green communications is to utilize interference signals as an energy supply for electronic devices. In this scenario, simultaneous wireless information and power transfer (SWIPT) schemes are a common technique to harvest energy from wireless signals. This paper addresses a performance comparison of different IA algorithms to guarantee the best trade-off between sum-rate and the amount of harvested energy, with an in-depth analysis.**

***Index Terms*—Interference alignment, Simultaneous Wireless Information and Power Transfer, Energy Harvesting, Green Communications.**

I. Introduction

INTERFERENCE management is one of the major challenges in actual cellular networks due to the dense deployment of small cells. Several traditional methods have been implemented to cancel interference such as Frequency-division multiple access (FDMA), Time-division multiple access (TDMA), treating the weak interference as noise, etc [1]. However, avoiding interference by orthogonalizing the channel access (TDMA, FDMA) does not optimally exploit the degrees of freedom (DoFs) of the communication system because each user only accesses to a fraction of all dimension (time/frequency). In this scenario, Interference Alignment (IA) has emerged as a promising solution with optimal DoFs performance. This means that it can reach the capacity of interference networks at a very high signal-to-noise ratio (SNR) [2], [3].

The main idea of IA is to cooperatively design the precoding and decoding matrices of all network users such that interference signals are constrained into certain subspaces orthogonal to the decoding matrix at the unintended receiver. Therefore, leaving some receiver dimensions free of interference for the desired signal. Interference could be aligned in different dimensions (time, frequency or spatial). However, spatial IA is the most widely used method taking advantage of multiple antennas in multiple-input multiple-output (MIMO) systems. IA has been applied in several networks provided its great performance, e.g, K-users MIMO interference networks, MIMO orthogonal frequency division multiplexing (MIMO-OFDM) channels, heterogeneous cellular networks and Cognitive Radio networks [4].

Nevertheless, there are several challenges for applying IA in practical systems. The closed-form solution of IA is an open problem for networks with more than three users. Therefore, iterative algorithms are developed to obtain IA solutions [5]–[7]. In addition, the global channel state information (CSI) should be available at each node. So, different algorithms have been designed to reduce the overhead of CSI feedback. In [5] an algorithm to minimize interference leakage (MIN-IL) and another to maximize signal to interference and noise ratio (MAX-SINR) are developed to work with only local knowledge of CSI. In [6] two robust methods based on mean squared error (MSE) namely SUM-MSE and MIN-MAX-MSE, are designed to achieve a high performance considering error in the CSI estimation. SUM-MSE minimizes the total MSE of the network under individual transmit power constraints while MIN-MAX-MSE minimizes the maximum MSE of each user. Blind IA (BIA) algorithms without any knowledge of CSI are developed in [8]–[10]. On the other hand, the complexity and convergence rate of the IA algorithms are other issues that limit their use in practical scenarios. To overcome this problem, an adaptation of MIN-IL based on the Gauss-Newton method (GN-IL), is proposed in [7] to increase the convergence rate. Performance degradation at low and moderate SNRs is another challenge in practical IA networks. In [11] a deep analysis of this problem is conducted and an Opportunistic Interference Alignment (OIA) scheme based on antenna switching is proposed.

Although IA algorithms have been designed to cancel interference, a recent assumption in green communications is to utilize these interference signals as an energy supply for self-sufficient wireless nodes [4]. Therefore, completely eliminating interference, instead of re-utilizing it to power electronic devices, is considered a great waste of energy. In this scenario, simultaneous wireless information and power transfer (SWIPT) schemes are a common technique to harvest

This work has received funding from the European Union (EU) Horizon 2020 research and innovation programme under the Marie Skłodowska-Curie ETN TeamUp5G, grant agreement No. 813391. Also, this work has been supported in part by the Spanish National Project TERESA-ADA, funded by (MINECO/AEI/FEDER, UE) under grant TEC2017-90093-C3-2-R.

energy from wireless signals, based on the principle that RF signals carry information and energy simultaneously [12], [13]. The main idea of SWIPT-IA systems is to divide the received signal to fed two different terminals: information decoder (ID) and energy harvester (EH). In the ID terminal interference is completely eliminated by IA decoding matrix while in EH terminal all received signal comprised by interference plus desired information is converted to electrical energy.

There are two classical receiver architectures for SWIPT to divide the received signal, i.e., time-switching (TS) and power-splitting (PS). When TS mode is adopted, a time switcher commute periodically the received signal into the two terminals. On the other hand, PS mode divides the received signal into two power streams for ID and EH simultaneously. PS is more suitable to be utilized in practical systems because it achieves the best trade-off between transmission rate and harvested energy and does not require accurate time synchronization [14].

The major challenge is how to balance ID and EH performance. Several solutions have been proposed to jointly optimize wireless energy harvesting (WEH) and IA based on user selection scheme [15] [16] [4], power allocation policies (PA) [17], angle switching (AS) schemes [18], power splitting optimization (PSO) algorithms [4], etc. PSO algorithms are addressed to find the optimum value of the portion of signal power that is split into the ID terminal, given by parameter ρ, to jointly maximize the sum-rate and harvested power.

In this paper, we study a K-user MIMO IA network with WEH capabilities based on a PS architecture incorporated at each receiver. We address a performance comparison of different IA algorithms (MIN-IL, GN-IL, MAX-SINR, and SUM-MSE), not available in the literature yet, in order to evaluate the join interference suppression and harvested power capacity of the IA-WEH networks. A deep analysis is conducted to evaluate the sum-rate, amount of harvested power and interference leakage of the IA algorithms over different values of SNR and ρ. The rate-energy trade-off is considered and we derive the general equations to compute sum-rate and harvested power considering different data streams. Numerical results illustrate the great interference suppression performance of the IA algorithms. On the other hand, simulations in practical scenarios show harvested power values that guarantee self-sustainable operations for low power consumption wireless nodes.

This paper is organized as follows. The system model and feasibility conditions of IA algorithms are presented in Section II. In Section III, a brief description of different IA algorithms (MIN-IL, GN-IL, MAX-SINR, and SUM-MSE) is conducted. Expressions of performance metrics for computing sum-rate and harvested power are derived in Section IV. Simulations results are illustrated in Section V to validate IA algorithms performance. Finally, Section VI concludes the paper.

Notation: boldface lower-case letters are used for vectors, while boldface upper-case letters are used for matrices. Tr($\mathbf{A}$), rank($\mathbf{A}$), $\mathbf{A}^T$, $\mathbf{A}^H$ and $\mathbf{A}^\dagger$, represent the trace, rank, transpose, Hermitian transpose and the Moore-Penrose pseudoinverse of matrix $\mathbf{A}$, respectively. vect($\mathbf{A}$) denotes the vector obtained by stacking the columns of $\mathbf{A}$ below one another, $\|\mathbf{a}\|$ denotes the Euclidean norm of $\mathbf{a}$ and $\|\mathbf{A}\|_F$ is the Frobenious norm of $\mathbf{A}$. $\mathbf{a}_{*l}$ represents the lth column vector of matrix $\mathbf{A}$. $\mathbb{C}^{M\times N}$ is the space of complex $M \times N$ matrices. $\mathcal{CN}\left(\mu, \sigma^2\right)$ is the complex Gaussian distribution with mean μ and variance σ^2. $\mathbb{E}(\cdot)$ stands for expectation. $\mathbf{I}_d$ represents the $d \times d$ identity matrix.

II. System model

We consider a K-user MIMO interference channel, where each kth transmitter, equipped with $M^{[k]}$ antennas, is intended to transmit $d^{[k]}$ data streams to its corresponding receiver, equipped with $N^{[k]}$ antennas. However, the transmission of the kth transmitter-receiver pair causes interference to the other $K-1$ receivers. Fig.1 shows an IA interference network with a PS architecture incorporated at the receiver side to harvest energy from RF signals. Each receiver implements the PS technique to divide the received signal power into two branches, for ID and EH terminals. After splitting the power, then the IA is applied in the ID branch in order to remove the interference. A remarkable feature of this scheme, shown in Fig. 1, is that, in the EH branch, all power including both desired signal and interference, are used for harvesting operation.

To avoid interference, IA algorithms design carefully the precoding matrix $\mathbf{V}^{[k]} \in \mathbb{C}^{M^{[k]}\times d^{[k]}}$ and the decoding matrix $\mathbf{U}^{[k]} \in \mathbb{C}^{N^{[k]}\times d^{[k]}}$. $\mathbf{V}^{[k]}$ is designed to restrict all the interference signals into a subspace orthogonal to $\mathbf{U}^{[k]}$, while the desired signal is allocated into another subspace free from interference. Therefore, the received signal at kth receiver in the ID terminal can be modeled as [17]:

$$\begin{aligned}\hat{\mathbf{y}}_{ID}^{[k]} &= \sqrt{\rho^{[k]}}\mathbf{U}^{[k]H}\mathbf{H}^{[k,k]}\mathbf{V}^{[k]}\mathbf{x}^{[k]} \\ &+\sqrt{\rho^{[k]}}\left(\sum_{j=1,j\neq k}^{K}\mathbf{U}^{[k]H}\mathbf{H}^{[k,j]}\mathbf{V}^{[j]}\mathbf{x}^{[j]}+\mathbf{U}^{[k]H}\mathbf{n}^{[k]}\right) \\ &+\mathbf{U}^{[k]H}\mathbf{z}^{[k]}, \quad k\in\{1,...,K\}\end{aligned} \tag{1}$$

where $\rho^{[k]} \in [0,1]$ is the portion of the received signal power derived to ID terminal, $\mathbf{x}^{[k]} \in \mathbb{C}^{d^{[k]}\times 1}$ are the transmitted symbols over $d^{[k]}$ data streams, $\mathbf{H}^{[k,j]} \in \mathbb{C}^{N^{[k]}\times M^{[j]}}$ represents the channel coefficients between jth transmitter and kth receiver ; $\mathbf{n}^{[k]} \in \mathbb{C}^{N^{[k]}\times 1}$ is the circularly symmetric additive white Gaussian antenna noise (AWGN) vector at kth receiver $\left(\mathbf{n}^{[k]} \sim \mathcal{CN}\left(0, \sigma^2\mathbf{I}_{N^{[k]}}\right)\right)$, and $\mathbf{z}^{[k]} \in \mathbb{C}^{N^{[k]}\times 1}$ represents the additional circuit noise due to non-ideal RF-to-baseband signal conversion and thermal noise, $\left(\mathbf{z}^{[k]} \sim \mathcal{CN}\left(0, \delta^2\mathbf{I}_{N^{[k]}}\right)\right)$ [17]. The transmitted signal power at jth transmitter is given by $P^{[j]} = \mathbb{E}\left[\left\|\mathbf{x}^{[j]}\right\|^2\right]$.

On the other hand, the received signal at EH terminal is modeled as [17]:

$$\hat{\mathbf{y}}_{EH}^{[k]} = \sqrt{1-\rho^{[k]}}\left(\sum_{j=1}^{K}\mathbf{H}^{[k,j]}\mathbf{V}^{[j]}\mathbf{x}^{[j]}+\mathbf{n}^{[k]}\right). \quad k\in\{1,...,K\} \tag{2}$$

IA algorithms have to satisfy the following feasibility conditions to suppress the interference and recover the desired signals. Condition (3) is related to the capacity of IA algorithms to cancel interference signals, while condition (4) expresses the capacity to recover all the desired symbols from $d^{[k]}$ data streams as:

$$\mathbf{U}^{[k]^H}\mathbf{H}^{[k,j]}\mathbf{V}^{[j]} = 0,\ \forall j \neq k, \tag{3}$$

$$rank(\mathbf{U}^{[k]^H}\mathbf{H}^{[k,k]}\mathbf{V}^{[k]}) = d^{[k]},\ \forall k. \tag{4}$$

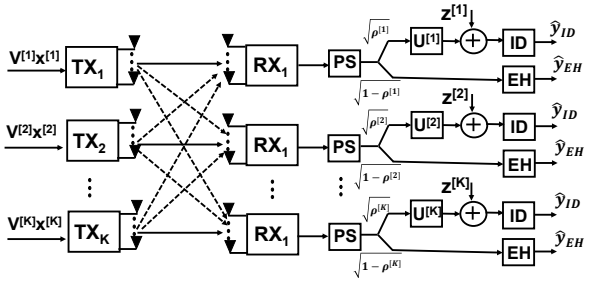

Fig. 1. K-user Interference MIMO Channel for SWIPT with both ID and EH terminals through a power splitter at each receiver

III. IA Algorithms

Several iterative algorithms have been proposed to obtain precoding and decoding matrices $\mathbf{V}^{[k]}$ and $\mathbf{U}^{[k]}$ to satisfy conditions (3) and (4). This section summarizes the main ideas behind different IA algorithms without considering SWIPT schemes (i.e. $\rho^{[k]} = 1$).

A. Minimization of Interference Leakage (MIN-IL)

An alternating algorithm based on the reciprocity of wireless networks is proposed in [5] to minimize the Interference Leakage (IL) at each receiver. IL is defined as the residual interference power in the received signal and it is computed as [5]:

$$I^{[k]} = \sum_{j=1,j\neq k}^{K}\left(\frac{P^{[j]}}{d^{[j]}}\left\|\mathbf{U}^{[k]^H}\mathbf{H}^{[k,j]}\mathbf{V}^{[j]}\right\|_F^2\right) = \mathrm{Tr}\left[\mathbf{U}^{[k]^H}\mathbf{Q}^{[k]}\mathbf{U}^{[k]}\right], \tag{5}$$

where $\mathbf{Q}^{[k]}$ is the interference covariance matrix at kth receiver [5]:

$$\mathbf{Q}^{[k]} = \sum_{j=1,j\neq k}^{K}\frac{P^{[j]}}{d^{[j]}}\mathbf{H}^{[k,j]}\mathbf{V}^{[j]}\mathbf{V}^{[j]^H}\mathbf{H}^{[k,j]^H}. \tag{6}$$

This means that each receiver has to identify the directions along which it receives the least interference [5] [3]. Therefore, $\mathbf{U}^{[k]}$ is computed as the eigenvector corresponding to the dth smallest eigenvalue, denoted as $\nu_d[\cdot]$, of $\mathbf{Q}^{[k]}$ $\left(\mathbf{U}^{[k]} = \nu_d[\mathbf{Q}^{[k]}],\ d = 1, ..., d^{[k]}\right)$. Then $\mathbf{V}^{[k]}$ is obtained as the eigenvector corresponding to the dth smallest eigenvalue of $\overleftarrow{\mathbf{Q}}^{[k]}$, which represents the interference covariance matrix in the reciprocal network. Matrices $\mathbf{U}^{[k]}$ and $\mathbf{V}^{[k]}$ are unitary $\left(\mathbf{U}^{[k]^H}\mathbf{U}^{[k]} = \mathbf{I}_d, \mathbf{V}^{[k]^H}\mathbf{V}^{[k]} = \mathbf{I}_d\right)$, whose columns form orthonormal basis of the interference-free desired signal subspace at kth receiver . This algorithm iteratively reduces the value of $I^{[k]}$ and values very close to zero are reached. However, due the nonconvex nature of the optimization problem, the convergence to a global minimum is not guaranteed. A distributed implementation of this algorithm which only needs local knowledge of CSI is also proposed in [5].

B. Gauss-Newton interference leakage (GN-IL)

This algorithm is an adaptation of MIN-IL solution to increase the convergence rate to minimize IL. MIN-IL is based on an alternating optimization procedure, while GN-IL applies a traditional Gauss-Newton method to minimize IL through a quadratic approximation of the objective function, which guarantees a quadratic convergence rate [7].

Let be $\mathbf{s} = [vec(\mathbf{V}^{[1]})^T, ..., vec(\mathbf{V}^{[K]})^T, ...vec(\mathbf{U}^{[1]^H})^T, ..., vec(\mathbf{U}^{[K]^H})^T]$ the column vector of all optimization variables with dimension $N_v = \sum_{k=1}^{K}\left(M^{[k]} + N^{[k]}\right)d^{[k]}$. Let be $r(\mathbf{s}) = \left[\mathbf{r}^{[1,2]^T}, \mathbf{r}^{[1,3]^T} ..., \mathbf{r}^{[K,(K-1)]^T}\right]^T$ the residual function computed as $\mathbf{r}^{[k,j]} = vec\left(\mathbf{U}^{[k]H}\mathbf{H}^{[k,j]}\mathbf{V}^{[j]}\right)$ and with dimension $N_e = \sum_{j=1,j\neq k}^{K} d^{[k]}d^{[j]}$. Then, $f(\mathbf{s}) = r(\mathbf{s})^H r(\mathbf{s}) : \mathbb{C}^{N_v} \to \mathbb{R}$ is the IL objective function. GN-IL proposes a second-order approximation of $f(\mathbf{s})$ and an iterative updating method of $\mathbf{s}$ to find the root of $f(\mathbf{s})$. The updating vector of $\mathbf{s}$ in the nth iteration is computed as $\Delta\mathbf{s}_n = -\mathbf{J}_{\mathbf{s}_n}^{\dagger} r(\mathbf{s}_n)$, where $\mathbf{s}_n$ is the value of $\mathbf{s}$ in the nth iteration, $\mathbf{J}_{\mathbf{s}_n}$ is the Jacobian matrix of $r(\mathbf{s}_n)$. $\Delta\mathbf{s}_n$ is comprised by the updating vector for $\mathbf{V}^{[k]}$ and $\mathbf{U}^{[k]}$ matrices. Then, both matrices are projected back to the Stiefel manifold through orthonormalization operations [7]. Therefore, this algorithm iteratively update $\mathbf{V}^{[k]}$ and $\mathbf{U}^{[k]}$ unitary matrices to minimize IL, but with higher convergence rate than MIN-IL.

C. MAX-SINR

MIN-IL algorithm does not consider the direct channel gain or noise power. Therefore, it achieves optimal performance as the SNR approaches to infinity but poor performance for low and intermediate SNR values. However, in practical systems low and intermediate SNR values are essential for several applications, especially at cell edge. Therefore, a MAX-SINR algorithm is proposed in [5], to improve the performance of MIN-IL in lower SNR region. In this case, an alternating maximization of SINR method is developed to optimize both direct signal power and IL. The SINR at kth receiver and lth data stream is computed as [5]:

$$SINR^{[k,l]} = \frac{\mathbf{u}_{*l}^{[k]^H}\mathbf{H}^{[k,k]}\mathbf{v}_{*l}^{[k]}\mathbf{v}_{*l}^{[k]^H}\mathbf{H}^{[k,k]^H}\mathbf{u}_{*l}^{[k]}}{\mathbf{u}_{*l}^{[k]^H}\mathbf{B}^{[k,l]}\mathbf{u}_{*l}^{[k]}}\frac{P^{[k]}}{d^{[k]}}, \tag{7}$$

where $\mathbf{B}^{[k,l]}$ is the interference plus noise covariance matrix at kth receiver and lth data stream :

$$\mathbf{B}^{[k,l]} = \sum_{j=1}^{K} \frac{P^{[j]}}{d^{[j]}} \mathbf{H}^{[k,j]} \mathbf{V}^{[j]} \mathbf{V}^{[j]H} \mathbf{H}^{[k,j]H} - \frac{P^{[k]}}{d^{[k]}} \mathbf{H}^{[k,k]} \mathbf{v}_{*l}^{[k]} \mathbf{v}^{[k]H}_{*l} \mathbf{H}^{[k,k]H} + \left(\sigma^2 + \delta^2\right) \mathbf{I}_{N^{[k]}}, \tag{8}$$

Therefore, the unit vector $\mathbf{u}_{*l}^{[k]}$, that maximizes $SINR^{[k,l]}$, is given by $\mathbf{u}_{*l}^{[k]} = \frac{\left(\mathbf{B}^{kl)}\right)^{-1} \mathbf{H}^{[k,k]} \mathbf{v}_{*l}^{[k]}}{\left\| \left(\mathbf{B}^{kl)}\right)^{-1} \mathbf{H}^{[k,k]} \mathbf{v}_{*l}^{[k]} \right\|}$. Then $\mathbf{V}^{[k]}$ is obtained in a similar way, but considering the $\overleftarrow{\mathbf{B}}^{[k,l]}$ matrix in the reciprocal network. The convergence rate of this method is an open problem [5]. In addition, similar to MIN-IL, a distributed implementation of MAX-SINR with only local knowledge of CSI, is also proposed in [5].

D. SUM-MSE

This algorithm is an improved version of MAX-SINR to increase the performance for low and moderate SNR values. The objective function is the total mean squared error (MSE) [6]:

$$\begin{aligned} &\min_{\mathbf{V}^{[k]}, \mathbf{U}^{[k]}} && \sum_{k=1}^{K} MSE^{[k]} \\ &s.t. && \mathrm{Tr}\left(\mathbf{V}^{[k]H} \mathbf{V}^{[k]}\right) \leq P^{[k]} \qquad k \in \{1, ..., K\} \end{aligned} \tag{9}$$

where $MSE^{[k]} = \mathbb{E}\left[\left\|\hat{\mathbf{y}}^{[k]} - \mathbf{x}^{[k]}\right\|^2\right]$ and a power constraint is imposed being $\mathrm{Tr}\left(\mathbf{V}^{[k]H} \mathbf{V}^{[k]}\right) = \left\|\mathbf{V}^{[k]}\right\|_F^2$ the transmitted signal power assuming that $\mathbb{E}\left[\left\|\mathbf{x}^{[k]}\right\|^2\right] = 1$. Lagrange optimization method is applied to obtain the expressions to compute $\mathbf{V}^{[k]}$ and $\mathbf{U}^{[k]}$:

$$\mathbf{V}^{[k]} = \left(\sum_{j=1}^{K} \mathbf{H}^{[k,j]H} \mathbf{U}^{[j]} \mathbf{U}^{[j]H} \mathbf{H}^{[k,j]} + \lambda^{[k]} \mathbf{I}_{M^{[k]}}\right)^{-1} \cdot \mathbf{H}^{[k,k]H} \mathbf{U}^{[k]}, \tag{10}$$

$$\mathbf{U}^{[k]H} = \mathbf{V}^{[k]H} \mathbf{H}^{[k,k]H} \cdot \left(\sum_{j=1}^{K} \mathbf{H}^{[k,j]} \mathbf{V}^{[j]} \mathbf{V}^{[j]H} \mathbf{H}^{[k,j]H} + \left(\sigma^2 + \delta^2\right) \mathbf{I}_{N^{[k]}}\right)^{-1}, \tag{11}$$

where $\lambda^{[k]}$ is the Lagrange multiplier associated with the power constraint of the kth transmitter and it is numerically solved such that the power constraint is satisfied with equality $\mathrm{Tr}\left(\mathbf{V}^{[k]}\left(\lambda^{[k]}\right)^H \mathbf{V}^{[k]}\left(\lambda^{[k]}\right)\right) = P^{[k]}$.

According to (10) and (11), optimal matrix $\mathbf{V}^{[k]}$ for each user depends on the optimal matrix $\mathbf{U}^{[k]}$ for all users, and vice versa. Therefore, the main idea is to iteratively update $\mathbf{V}^{[k]}$ and $\mathbf{U}^{[k]}$ matrices by using (10) and (11) to minimize MSE. In addition, an adaptation of this algorithm is also proposed in [6] assuming error in the CSI estimation. A detailed description of the convergence of these methods is included in [6].

IV. Join analysis of sum-rate and harvested power

Sum-rate and harvested power are the main performance metrics for IA networks with WEH capabilities. Rate-energy trade-off optimization is the major concern in WEH networks [19]. The rate achieved at kth receiver can be computed as [6], [17]:

$$R^{[k]} = \sum_{l=1}^{d^{[k]}} \log_2\left(1 + SINR^{[k,l]}\right), \tag{12}$$

where $SINR^{[k,l]}$ is the signal-to-interference-plus-noise ratio (SINR) at kth receiver and lth data stream and it is computed similar to (7) as follows:

$$SINR^{[k,l]} = \frac{P^{[k]} \rho^{[k]}}{d^{[k]}} \frac{\mathbf{u}^{[k]}_{*l}{}^H \mathbf{H}^{[k,k]} \mathbf{v}_{*l}^{[k]} \mathbf{v}^{[k]}_{*l}{}^H \mathbf{H}^{[k,k]H} \mathbf{u}_{*l}^{[k]}}{\mathbf{u}^{[k]}_{*l}{}^H \mathbf{B}^{[k,l]} \mathbf{u}_{*l}^{[k]}}, \tag{13}$$

where $\mathbf{B}^{[k,l]}$ is given by:

$$\mathbf{B}^{[k,l]} = \rho^{[k]} \sum_{j=1}^{K} \frac{P^{[j]}}{d^{[j]}} \mathbf{H}^{[k,j]} \mathbf{V}^{[j]} \mathbf{V}^{[j]H} \mathbf{H}^{[k,j]H} - \rho^{[k]} \left(\frac{P^{[k]}}{d^{[k]}} \mathbf{H}^{[k,k]} \mathbf{v}_{*l}^{[k]} \mathbf{v}^{[k]H}_{*l} \mathbf{H}^{[k,k]H} + \sigma^2 \mathbf{I}_{N^{[k]}}\right) + \delta^2 \mathbf{I}_{N^{[k]}}. \tag{14}$$

Then, the sum-rate is computed as:

$$R = \sum_{k=1}^{K} R^{[k]}. \tag{15}$$

On the other hand, the total amount of harvested power at kth receiver is computed as [17]:

$$P_h^{[k]} = \zeta\left(1 - \rho^{[k]}\right) \sum_{j=1}^{K} \frac{P^{[j]}}{d^{[j]}} \left\|\mathbf{H}^{[k,j]} \mathbf{V}^{[j]}\right\|_F^2, \tag{16}$$

where $0 < \zeta < 1$ is the energy conversion efficiency for converting the harvested energy to electrical energy to be stored. In this case, we consider the noise power is negligible for energy harvesting applications, as commonly assumed [17].

V. Simulation results

Simulations are performed for $K = 3$ users in a MIMO IA symmetric network, i.e, $M^{[k]} = N_t, N^{[k]} = N_r$, and $d^{[k]} = d$, $\forall k \in \{1, ..., K\}$. We consider $N_t = N_r = 4$ and $d = 2$. We also consider for simplicity perfect global knowledge of CSI and $\rho^{[k]} = \rho$, $\forall k \in \{1, ..., K\}$. We assume a Rayleigh block fading channel, where each entry of $\mathbf{H}^{[k,j]}$ is assumed to be independent and identically distributed (i.i.d), $\mathbf{H}^{[k,j]} \sim \mathcal{CN}\left(0, 10^{-4}\right)$, which corresponds to a path loss of 40 dB [17]. We also consider $\sigma^2 = -70$ dBm, $\delta^2 = -50$ dBm and $\zeta = 0.5$ [17]. We average all results over 100 channel realizations.

Figures 2 and 3 are obtained for $\rho = 1$ to illustrate the maximum capacity achieved by the IA-network. Fig. 2 depicts the average sum-rate for the studied IA algorithms over a SNR range [0, 40] dB. MIN-IL and GN-IL achieve similar sum-rate values for all SNR range, but MIN-IL requires 1328 iterations while GN-IL only employs 14 iterations. This result

shows the higher convergence rate of GN-IL algorithm. On the other hand, MAX-SINR and SUM-MSE also achieve similar values of sum-rate for all SNR range. However, SUM-MSE requires more simulation time than MAX-SINR because SUM-MSE numerically solves the Lagrange multiplier $\lambda^{[k]}$ in each iteration to satisfy the power constraint. MIN-IL and GN-IL only achieves better performance than MAX-SINR and SUM-MSE for high values of SNR (SNR>35 dB). Therefore, the performance improvement of MAX-SINR and SUM-MSE for low and moderate SNR values is proved numerically.

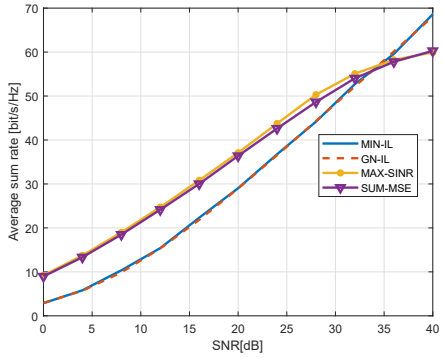

Fig. 2. Average sum-rate for different IA algorithms and different values of SNR, assuming $\rho = 1$.

In Fig. 3 a comparison of IL values is illustrated. MIN-IL and GN-IL achieve great interference suppression performance as suggested their theoretical formulation. However, MAX-SINR and SUM-MSE do not reach the same IL values because they are designed to maximize SINR and minimize MSE, respectively, instead of only reducing IL. Interference suppression performance remains almost constant for the entire SNR range in each algorithm.

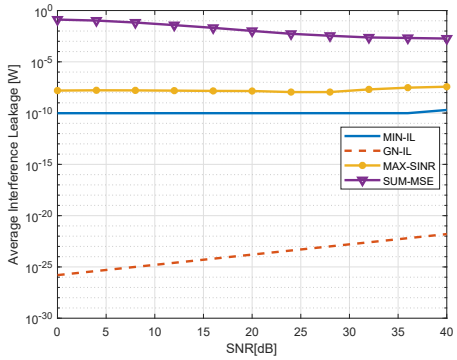

Fig. 3. Average interference leakage for different IA algorithms and different values of SNR, assuming $\rho = 1$.

Fig. 4 exhibits the average harvested power values for each user of the network assuming $\rho = 0$. Similar values are obtained for each IA algorithm because, as suggested by (16), $P_h^{[k]}$ only depends on transmitted power, channel gain and technological constant ζ. These harvested power values are enough to guarantee a self-sustainable operation for low power consumption nodes as wireless sensor nodes [20].

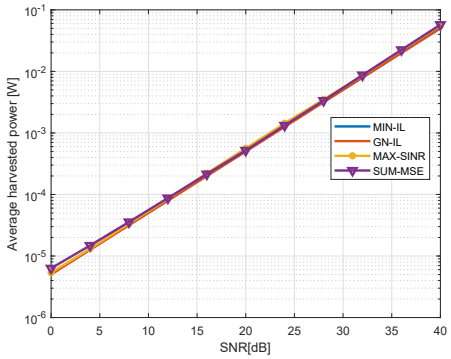

Fig. 4. Average harvested power for different IA algorithms and different values of SNR, assuming $\rho = 0$ and $\zeta = 0.5$.

Then, Figures 5-7 show the average sum-rate, the average harvested power and the average IL for different values of $\rho \in [0, 1]$ assuming SNR=20 dB, respectively. Fig. 5 illustrates that MAX-SINR and SUM-MSE achieve higher performance than MIN-IL and GN-IL, for SNR=20 dB and for all ρ values. As the parameter ρ gets higher means that the ID terminal has priority over the EH terminal. Therefore, the sum-rate increases while the harvested power decreases. According to Fig. 4, a similar amount of harvested power is obtained in Fig. 6 for each IA algorithm.

Figures 5 and 6 prove the theoretical proposition developed in [19], which states that the optimal rate-energy trade-off is achieved when $\rho \to 0$. The main reason to justify this behavior is that ID and EH terminals operate with very different power sensitivity (e.g., -10dBm for EH and -60dBm for ID) [19]. Finally, Fig. 7 exhibits the great interference suppression capacity achieved by every IA algorithm for all ρ values.

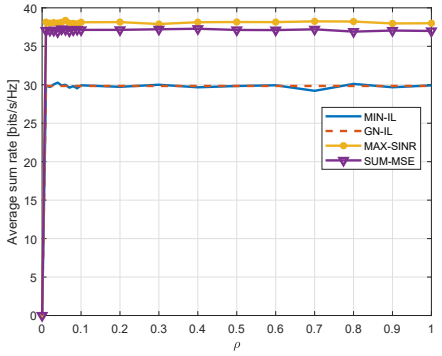

Fig. 5. Average sum-rate for different IA algorithms and different values of ρ, assuming SNR=20 dB.

VI. Conclusions

In this paper, we address a performance comparison of different IA algorithms (MIN-IL, GN-IL, MAX-SINR and SUM-MSE) over a K-user MIMO interference channel with

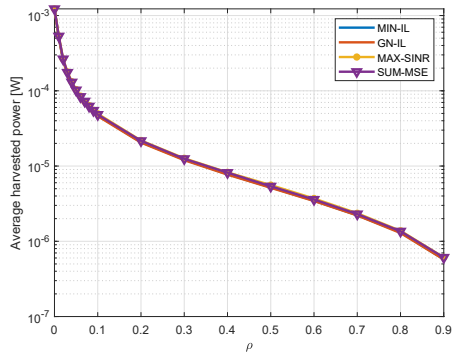

Fig. 6. Average harvested power for different IA algorithms and different values of ρ, assuming SNR=20 dB and $\zeta = 0.5$.

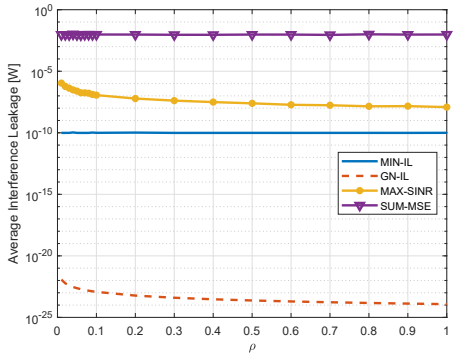

Fig. 7. Average interference leakage for different IA algorithms and different values of ρ, assuming SNR=20 dB.

WEH capabilities. Sum-rate, interference leakage, and harvested power are used as performance metrics. We illustrate that MIN-IL and GN-IL achieve higher interference suppression capacity than MAX-SINR and SUM-MSE over all SNR range. However, GN-IL and MIN-IL sum-rate performance is only superior than MAX-SINR and SUM-MSE for high SNR values. On the other hand, the amount of harvested power obtained in each algorithm is quite similar. Therefore, MAX-SINR and SUM-MSE are more suitable for cell edge applications. We show that IA algorithms achieve great interference suppression and SWIPT scheme allows to re-utilize these interference signals to power self-sufficient wireless nodes. Simulations results illustrate harvested power values that guarantee self-sustainable operations for low power consumption wireless nodes. IA-WEH network is a promising solution to satisfy the traffic demand free from interference in actual cellular networks while green communication requirements are guaranteed. Future works may be conducted to analyze the influence in the performance metrics of imperfect CSI estimation.

REFERENCES

[1] N. Zhao, F. R. Yu, M. Jin, Q. Yan, and V. C. M. Leung, "Interference Alignment and Its Applications: A Survey, Research Issues, and Challenges," *IEEE Communications Surveys Tutorials*, vol. 18, no. 3, pp. 1779–1803, 2016.

[2] V. R. Cadambe and S. A. Jafar, "Interference Alignment and Degrees of Freedom of the K-User Interference Channel," *IEEE Transactions on Information Theory*, vol. 54, no. 8, pp. 3425–3441, Aug. 2008.

[3] S. A. Jafar, "Interference Alignment: A New Look at Signal Dimensions in a Communication Network," *Foundations and Trends in Communications and Information Theory*, vol. 7, no. 1, pp. 1–130, 2010.

[4] N. Zhao, F. R. Yu, and V. C. Leung, "Wireless energy harvesting in interference alignment networks," *IEEE Communications Magazine*, vol. 53, no. 6, pp. 72–78, Jun. 2015.

[5] K. Gomadam, V. R. Cadambe, and S. A. Jafar, "A Distributed Numerical Approach to Interference Alignment and Applications to Wireless Interference Networks," *IEEE Transactions on Information Theory*, vol. 57, no. 6, pp. 3309–3322, Jun. 2011.

[6] H. Shen, B. Li, M. Tao, and X. Wang, "MSE-Based Transceiver Designs for the MIMO Interference Channel," *IEEE Transactions on Wireless Communications*, vol. 9, no. 11, pp. 3480–3489, Nov. 2010.

[7] O. González, C. Lameiro, and I. Santamaría, "A Quadratically Convergent Method for Interference Alignment in MIMO Interference Channels," *IEEE Signal Processing Letters*, vol. 21, no. 11, pp. 1423–1427, Nov. 2014.

[8] S. H. Chae and S.-Y. Chung, "Blind Interference Alignment for a Class of K-user Line-of-Sight Interference Channels," *IEEE Transactions on Communications*, vol. 60, no. 5, pp. 1177–1181, May 2012.

[9] M. M. Céspedes, J. Plata-Chaves, A. G. Armada, and L. Vandendorpe, "A blind interference alignment scheme for practical channels," in *2016 IEEE International Conference on Communications (ICC)*, May 2016, pp. 1–6.

[10] M. Morales-Céspedes, J. Plata-Chaves, D. Toumpakaris, S. A. Jafar, and A. G. Armada, "Cognitive Blind Interference Alignment for Macro-Femto Networks," *IEEE Transactions on Signal Processing*, vol. 65, no. 19, pp. 5121–5136, Oct. 2017.

[11] N. Zhao, F. R. Yu, H. Sun, A. Nallanathan, and H. Yin, "A Novel Interference Alignment Scheme Based on Sequential Antenna Switching in Wireless Networks," *IEEE Transactions on Wireless Communications*, vol. 12, no. 10, pp. 5008–5021, Oct. 2013.

[12] L. R. Varshney, "Transporting information and energy simultaneously," in *2008 IEEE International Symposium on Information Theory*, Jul. 2008, pp. 1612–1616.

[13] T. D. Ponnimbaduge Perera, D. N. K. Jayakody, S. K. Sharma, S. Chatzinotas, and J. Li, "Simultaneous Wireless Information and Power Transfer (SWIPT): Recent Advances and Future Challenges," *IEEE Communications Surveys Tutorials*, vol. 20, no. 1, pp. 264–302, 2018.

[14] N. Zhao, S. Zhang, F. R. Yu, Y. Chen, A. Nallanathan, and V. C. M. Leung, "Exploiting Interference for Energy Harvesting: A Survey, Research Issues, and Challenges," *IEEE Access*, vol. 5, pp. 10 403–10 421, 2017.

[15] N. Zhao, F. R. Yu, and V. C. Leung, "Opportunistic interference alignment networks for simultaneous wireless information and power transfer through user selection," in *2014 Sixth International Conference on Wireless Communications and Signal Processing (WCSP)*, Oct. 2014, pp. 1–5.

[16] ——, "Simultaneous wireless information and power transfer in interference alignment networks," in *2014 International Wireless Communications and Mobile Computing Conference (IWCMC)*, Aug. 2014, pp. 7–11.

[17] Z. Zong, H. Feng, F. R. Yu, N. Zhao, T. Yang, and B. Hu, "Optimal Transceiver Design for SWIPT in k-User MIMO Interference Channels," *IEEE Transactions on Wireless Communications*, vol. 15, no. 1, pp. 430–445, Jan. 2016.

[18] N. Zhao, F. R. Yu, and V. C. Leung, "Wireless power transfer based on angle switching in interference alignment wireless networks," in *2015 IEEE International Conference on Communications (ICC)*, Jun. 2015, pp. 3776–3781.

[19] X. Zhou, R. Zhang, and C. K. Ho, "Wireless Information and Power Transfer: Architecture Design and Rate-Energy Tradeoff," *IEEE Transactions on Communications*, vol. 61, no. 11, pp. 4754–4767, Nov. 2013.

[20] M.-L. Ku, W. Li, Y. Chen, and K. J. Ray Liu, "Advances in Energy Harvesting Communications: Past, Present, and Future Challenges," *IEEE Communications Surveys Tutorials*, vol. 18, no. 2, pp. 1384–1412, 2016.